Resolving the Mystery of X-Ray-Faint Elliptical Galaxies: Chandra X-Ray Observations of NGC 4697

Craig L. Sarazin – University of Virginia
Jimmy A. Irwin – University of Michigan
Joel N. Bregman – University of Michigan

Citation of published version:

Sarazin, C., Irwin, J., Bregman, J. (2000): Resolving the Mystery of X-Ray-Faint Elliptical Galaxies: Chandra X-Ray Observations of NGC 4697. *The Astrophysical Journal Letters*, 544(2). DOI: 10.1086/317308

THE ASTROPHYSICAL JOURNAL, 544:L101–L105, 2000 December 1

RESOLVING THE MYSTERY OF X-RAY–FAINT ELLIPTICAL GALAXIES: *CHANDRA* X-RAY OBSERVATIONS OF NGC 4697

CRAIG L. SARAZIN,[1] JIMMY A. IRWIN,[2,3] AND JOEL N. BREGMAN[2]
Received 2000 June 30; accepted 2000 September 27; published 2000 November 10

ABSTRACT

Chandra observations of the X-ray–faint elliptical galaxy NGC 4697 resolve much of the X-ray emission (61% within one effective radius) into ~80 point sources, of which most are low-mass X-ray binaries (LMXBs). These LMXBs provide the bulk of the hard emission and much of the soft emission as well. Of the remaining unresolved emission, it is likely that about half is from fainter LMXBs, while the other half (~23% of the total emission) is from interstellar gas. Three of the resolved sources are supersoft sources. In the outer regions of NGC 4697, eight of the LMXBs (about 25%) are coincident with candidate globular clusters, indicating that globulars have a high probability of containing X-ray binaries compared with the normal stellar population. The X-ray luminosities (0.3–10 keV) of the resolved LMXBs range from $\sim 5 \times 10^{37}$ to $\sim 2.5 \times 10^{39}$ ergs s^{-1}. The luminosity function of the LMXBs has a "knee" at 3.2×10^{38} ergs s^{-1}, which is roughly the Eddington luminosity of an 1.4 $M_\odot$ neutron star (NS); this knee might be useful as a distance indicator. The highest luminosity source has the Eddington luminosity of an ~20 $M_\odot$ black hole (BH). The presence of this large population of NS and massive BH stellar remnants in this elliptical galaxy shows that it (or its progenitors) once contained a large population of massive main-sequence stars.

Subject headings: binaries: close — galaxies: elliptical and lenticular, cD — galaxies: ISM — X-rays: galaxies — X-rays: ISM — X-rays: stars

1. INTRODUCTION

Observations with the *Einstein Observatory* showed that elliptical and S0 galaxies are luminous sources of X-ray emission (e.g., Forman, Jones, & Tucker 1985). At least for the X-ray–luminous early-type galaxies (defined as those having a relatively high ratio of X-ray to optical luminosity L_X/L_B), the bulk of the X-ray luminosity is from hot (~10^7 K) interstellar gas. However, there is a large dispersion in the X-ray luminosities of early-type galaxies of a given optical luminosity. We will refer to galaxies that have a very low L_X/L_B ratio as "X-ray faint." In these X-ray–faint elliptical galaxies, much of the hot interstellar gas may have been lost in galactic winds or by ram pressure stripping by ambient intracluster or intragroup gas. The source of the bulk of the X-ray emission in X-ray–faint galaxies is uncertain.

In general, X-ray–faint galaxies exhibit significantly different spectral properties than their X-ray–bright counterparts. The X-ray–bright galaxies are dominated by thermal emission at $kT \sim 0.8$ keV because of their hot interstellar medium (ISM). On the other hand, the X-ray–faint galaxies exhibit two distinct spectral components: first, they have a hard ~5–10 keV component, most easily seen in *ASCA* spectra (Matsumoto et al. 1997), which is roughly proportional to the optical luminosity of the galaxy. This suggests that the hard component is due to low-mass X-ray binaries (LMXBs) like those seen in the bulge of our Galaxy and M31. Second, X-ray–faint galaxies have a very soft (~0.2 keV) component, whose origin is uncertain (Fabbiano, Kim, & Trinchieri 1994; Pellegrini 1994; Kim et al. 1996). Suggested stellar sources for the very soft emission in X-ray–faint elliptical galaxies include active M stars, RS CVn binaries, or supersoft sources, but none of these appear to work quantitatively (Pellegrini & Fabbiano 1994; Irwin & Sarazin 1998b). It is possible that the soft X-rays are due to a warm (0.2 keV) ISM. Recently, we proposed that the very soft emission in X-ray–faint elliptical galaxies is due to the same LMXBs responsible for the hard emission (Irwin & Sarazin 1998a, 1998b). However, the origin of the very soft component in X-ray–faint elliptical galaxies remains something of a mystery.

With the superb spatial resolution of the *Chandra X-Ray Observatory*, it should be possible to resolve the emission from nearby X-ray–faint early-type galaxies into LMXBs, if this is indeed the source of their emission. Recently, we used a deep *ROSAT* HRI observation to detect a number of discrete X-ray sources in the X-ray–faint elliptical galaxy NGC 4697 (Irwin, Sarazin, & Bregman 2000). However, the bulk of the X-ray emission was not resolved. We also simulated a 40 ks *Chandra* observation of NGC 4697 and showed that it should be possible to detect ~100 LMXBs if they provide the bulk of the emission. Here we present the results of exactly this observation. At a distance of 15.9 Mpc (Faber et al. 1989; assuming a Hubble constant of 50 km s^{-1} Mpc^{-1}), NGC 4697 is the closest normal, optically luminous, X-ray–faint elliptical galaxy. Given its proximity, NGC 4697 is an ideal target for detecting the LMXB population. It is sufficiently X-ray faint that diffuse ISM emission should not bury the fainter LMXBs. The purposes of the *Chandra* observation are to resolve and study the LMXB population of NGC 4697, to determine the source of both the hard and soft spectral components, and to detect or place strong limits on any residual diffuse (possibly gaseous) emission.

2. X-RAY OBSERVATION

NGC 4697 was observed on 2000 January 15–16 with the *Chandra* Advanced CCD Imaging Spectrometer (ACIS) S3 detector for a total exposure of 39,434 s. The S3 chip was chosen because of its good low-energy response. No background flares occurred during this observation. This observation was processed at a time when the standard pipeline pro-

[1] Department of Astronomy, University of Virginia, P. O. Box 3818, Charlottesville, VA 22903-0818; cls7i@virginia.edu.
[2] Astronomy Department, University of Michigan at Ann Arbor, 830 Dennison, 501 East University Avenue, Ann Arbor, MI 48109-1090; jirwin@astro.lsa.umich.edu, jbregman@umich.edu.
[3] *Chandra* Fellow.

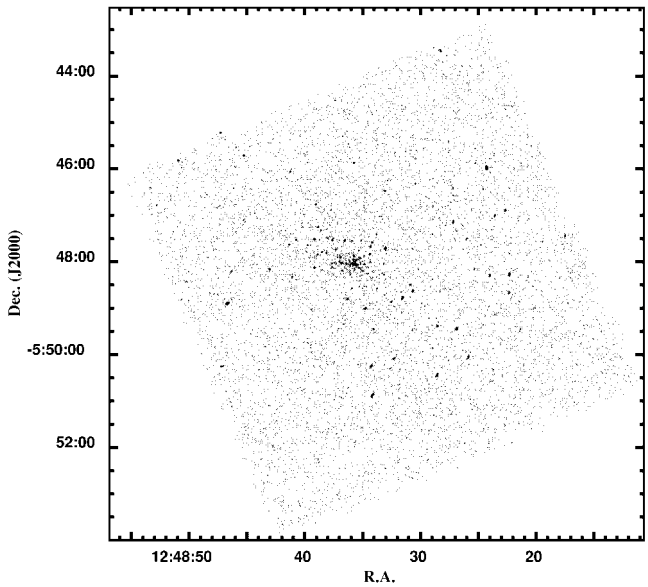

FIG. 1.—Entire *Chandra* S3 X-ray image of the region around NGC 4697 in the 0.3–10 keV band. The optical center of the galaxy is located at the center of the concentration of X-ray point sources to the northeast of the chip center.

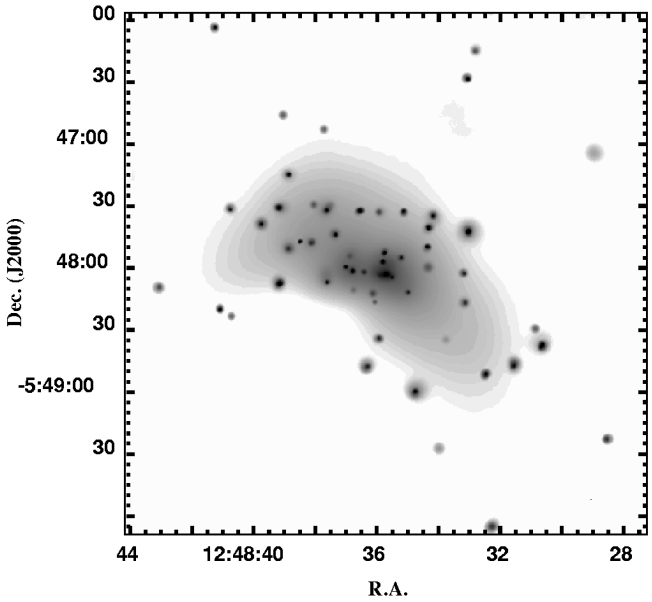

FIG. 2.—*Chandra* X-ray image of a $4' \times 4'$ region around NGC 4697 (0.3–10 keV). The image was adaptively smoothed to a minimum signal-to-noise ratio of 3 per smoothing beam and corrected for background and exposure. The gray scale is logarithmic and ranges from 8×10^{-7} to 4×10^{-3} counts arcsec^{-2} s^{-1}.

cessing introduced a boresight error of about 8″ in the absolute positions of X-ray sources. The absolute positions were corrected by using the optical identifications and positions from the USNO-A2.0 catalog (Monet et al. 1998) of X-ray sources. The absolute positions are accurate to about 0.″5 near the center of the S3 image, with larger errors farther out. Background was taken from the outer regions of the same chip and blank sky backgrounds. More details concerning the X-ray observation, data analysis, variability of the sources, and spectral fitting are given in C. L. Sarazin, J. A. Irwin, & J. N. Bregman (2000, in preparation, hereafter Paper II).

3. X-RAY IMAGE

The *Chandra* S3 chip X-ray image is shown in Figure 1. The central portion of the *Chandra* image (adaptively smoothed) is shown in Figure 2. These images show the basic result of the *Chandra* observation: much of the emission from the galaxy is resolved into individual point sources of X-rays (§ 4). However, Figure 2 indicates that there is also some unresolved, diffuse emission. The diffuse emission is centrally concentrated, and its X-ray surface brightness increases by about a factor of 30 into the center of the galaxy. Both the point sources and the diffuse emission are elongated in the same direction as this E6 galaxy (a position angle of 67°).

We determined the portion of the X-ray emission that is due to resolved sources and diffuse emission, both for the entire *Chandra* X-ray band (0.3–10 keV) and for three narrower bands: hard *H* (2–10 keV), medium *M* (1–2 keV), and soft *S* (0.3–1 keV). Here we report on the counts coming from within the elliptical optical isophote containing one-half of the optical light ("one effective radius," semimajor axis 95″, semiminor axis 55″). First, the population of resolved sources was determined as discussed below (§ 4). Then the total emission was determined, and the source flux subtracted, to give the amount of unresolved emission.

Within one effective radius, 61% of the X-ray emission is resolved into individual X-ray sources for the total band. In the hard, medium, and soft bands, the resolved fractions are 81%, 79%, and 48%, respectively. Thus, it is clear that the bulk of the total X-ray emission from NGC 4697 comes from point sources, which are likely to be LMXBs.

A portion of the unresolved emission must also come from LMXBs that fall below our threshold for reliable detection of resolved sources. Indeed, if one sets the detection threshold for sources lower, one finds many more 2 σ fluctuations than expected just from Poisson statistics. If the observed luminosity function of the resolved sources in NGC 4697 (Fig. 3) is extended down to $L_X \approx 10^{36}$ ergs s^{-1}, the approximate lower limit for LMXBs in globular clusters (Hertz & Grindlay 1983), the contribution of LMXBs to the total band X-ray emission from NGC 4697 increases to 74% within one effective radius. The X-ray spectrum of the diffuse emission is somewhat softer than that of the resolved sources. If one decomposes the unresolved emission into two components, one with the same spectrum as that of the sum of the resolved sources plus a softer component, one finds that the LMXBs would contribute about 77% of the total band emission.

The remaining ~23% of the emission would come from a more diffuse component with a soft (~0.3 keV) spectrum. This soft component has a very extended spatial distribution (Paper II) and is most likely due to interstellar gas. Additional evidence for ISM emission comes from the adaptively smoothed X-ray image (Fig. 2). If the diffuse X-ray emission is from a large number of faint stellar sources, then it should appear smooth and symmetrical (like the optical image). The diffuse emission in Figure 2 is smooth and fairly symmetric in the inner regions, but there is an extended asymmetrical feature at the outer regions to the northeast. Such asymmetries are more easily produced in the distribution of gas (e.g., by ram pressure) than in the distribution of stellar sources.

4. RESOLVED SOURCES

The discrete X-ray source population in the ACIS-S3 image (Fig. 1) was determined using a wavelet detection algorithm

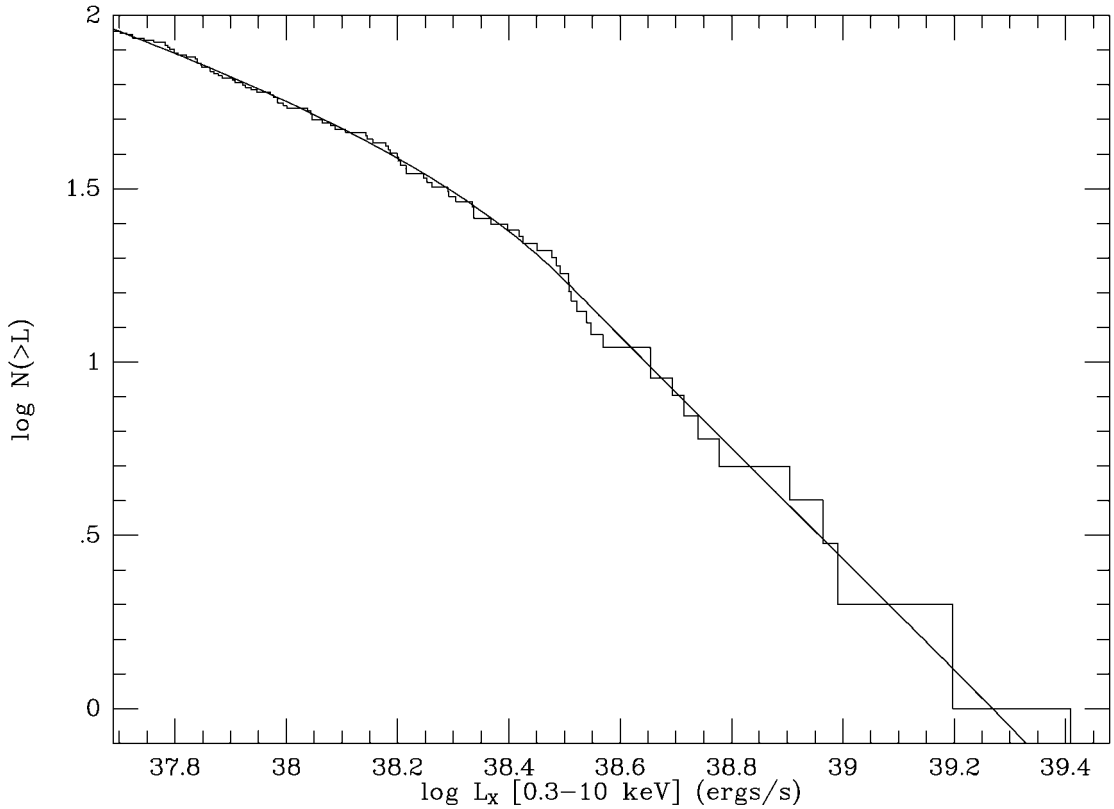

FIG. 3.—Histogram of the observed cumulative X-ray luminosity function of all resolved sources within the *Chandra* S3 field. The continuous curve is the sum of the best-fit LMXB luminosity function for NGC 4697 (eq. [1]) plus the expected background source counts.

with the source detection threshold set at 10^{-6}, which implies that $\lesssim 1$ false source (due to a statistical fluctuation in the background) would be detected in the entire S3 image. The minimum detectable flux was about 2.6×10^{-4} counts s^{-1} ($L_X = 5.0 \times 10^{37}$ ergs s^{-1} at the NGC 4697 distance) in the 0.3–10 keV band in the part of the chip covered by the galaxy. Fluxes were corrected for exposure and the instrument point-spread function. A total of 90 sources were found; a complete list with positions and other properties is given in Paper II.

Some of the detected sources are likely to be unrelated foreground or (more likely) background objects. Based on the source counts in Brandt et al. (2000) and Mushotzky et al. (2000), we would expect about 10–15 unrelated sources in our observation. The unrelated sources should mainly be found at larger distances from the optical center of NGC 4697, while the sources associated with NGC 4697 should be concentrated toward the center of the galaxy. Within 2′ of the center of NGC 4697 (roughly the region covered by Fig. 2), approximately three of the ~60 detected sources would be expected to be unrelated to NGC 4697.

Eight of the X-ray sources coincide (within 1″) with candidate globular clusters in NGC 4697. CXOU J124834.4−055014 (Paper II, source 64) is identified with globular cluster 33 in Hanes (1977), while CXOU J124846.8−054852 (Paper II, source 72; Irwin et al. 2000, source 11) is associated with Hanes globular cluster 24. Six additional X-ray sources (CXOU J124827.0−054925, CXOU J124826.1−054729, CXOU J124830.8−054836, CXOU J124834.2−054926, CXOU J124835.9−054551, and CXOU J124841.5−054736) are in positional agreement with the candidate globulars kindly provided by J. J. Kavelaars (2000, private communication). Given the positional agreement of the X-ray sources with the globular candidates, it is likely that all eight of these identifications are real. However, at the distance to NGC 4697, globular clusters are not resolved in ground-based optical images, and the candidate globulars were identified by luminosities and (possibly) colors. As a result, as many as half of them might be unrelated faint optical objects rather than globular clusters.

The count rates for the sources were converted into unabsorbed luminosities (0.3–10 keV) by assuming that all of the sources were at the distance of NGC 4697. Using the best-fit *Chandra* X-ray spectrum of the resolved sources (Paper II), the resulting X-ray luminosities range from about 5×10^{37} to 2.5×10^{39} ergs s^{-1} (calibration uncertainties might affect the luminosities by ~25%). The cumulative luminosity function of all of the sources is shown in Figure 3. Note that the luminosity function appears to have a knee at $L_X \approx 3 \times 10^{38}$ ergs s^{-1}. In fitting the luminosity function, we corrected for unrelated sources using the deep source counts (Brandt et al. 2000; Mushotzky et al. 2000), assuming that the shape of the number versus flux relation is that derived from *ROSAT* deep fields (Hasinger et al. 1998). A single power-law (plus the background contribution) fit to the luminosity function could be rejected at the greater than 95% confidence level. However, a broken power-law fit was successful:

$$\frac{dN}{dL_{38}} = N_0 \left(\frac{L_{38}}{L_b}\right)^{-\alpha}, \qquad (1)$$

with $\alpha = \alpha_l$ for $L_{38} \leq L_b$ and $\alpha = \alpha_h$ for $L_{38} > L_b$. Here L_{38} is the X-ray luminosity (0.3–10 keV) in units of 10^{38} ergs s^{-1}. The

best fit, determined by the maximum likelihood method, gave $N_0 = 8.0^{+7.1}_{-5.2}$, $\alpha_l = 1.29^{+0.36}_{-0.49}$, $\alpha_h = 2.76^{+1.81}_{-0.39}$, and a break luminosity of $L_b = 3.2^{+2.0}_{-0.8} \times 10^{38}$ ergs s^{-1} (Fig. 3). The errors (at the 90% confidence level) were determined by Monte Carlo simulations.

The break luminosity is similar to the Eddington luminosity for spherical accretion onto a $1.4\,M_\odot$ neutron star. This suggests that the sources with luminosities above this break are accreting black holes, while those below the break are predominantly neutrons stars. This would imply that NGC 4697 contains $\gtrsim$15 luminous X-ray binary systems containing black holes. If the more luminous of these systems ($L_X \sim 10^{39}$ ergs s^{-1}) are limited by the Eddington luminosity, they must contain fairly massive ($M \gtrsim 8\ M_\odot$) black holes.

We studied the crude spectral properties of the resolved sources by using hardness ratios (for full results and spectral analysis, see Paper II). Hardness ratios or X-ray colors have the advantage that they can be applied to weaker sources. Figure 4 plots H31 versus H21. For comparison, the hardness ratios (H21, H31) are (-0.38, -0.57) for all of the emission, (-0.69, -0.82) for the unresolved emission, and (-0.14, -0.37) for the sum of the sources, all within one effective radius.

There are three moderate-luminosity sources with hardness ratios of (-1, -1), which means that they have no detectable emission beyond 1 keV. These three sources are almost certainly supersoft sources (e.g., Kahabka & van den Heuvel 1997). There are three sources, one of which is the brightest source in the field, with values of ~(1, 1), all of which are located greater than 3.′5 from the center of NGC 4697. These are probably unrelated, strongly absorbed active galactic nuclei. There are eight sources near (0, -1) that essentially have no hard emission. Six of these sources are at large radii (>2.′2), which suggests that this population is also unrelated to NGC 4697. Most of the sources lie in a diagonal swath centered at about (-0.15, -0.40). These values are similar to but slightly harder than the integrated colors for the entire galaxy, but they are considerably harder than the values for the unresolved emission. The X-ray sources identified with globular cluster candidates have hardness ratios that are similar to other LMXBs, with the exception of CXOU J124834.4$-$055014, whose hardness ratios suggest that it is actually a background active galactic nucleus.

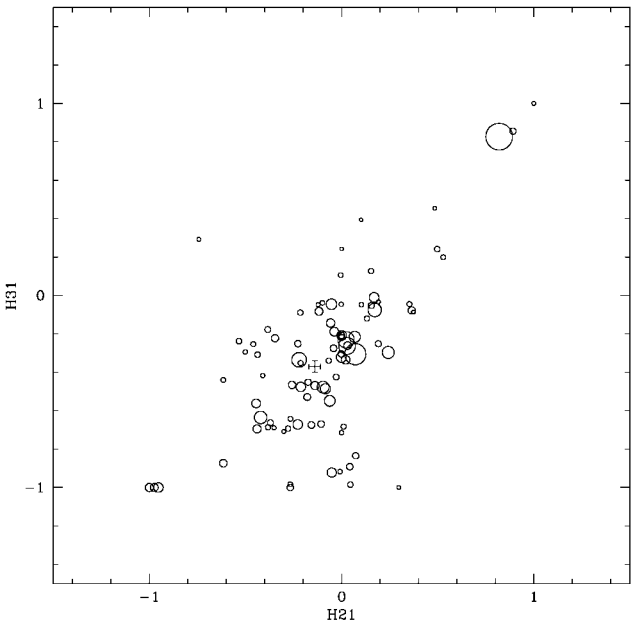

FIG. 4.—Hardness ratios for the NGC 4697 sources. Here H21 ≡ ($M - S$)/($M + S$) and H31 ≡ ($H - S$)/($H + S$), where S, M, and H are the counts in our soft (0.3–1 keV), medium (1–2 keV), and hard (2–10 keV) bands, respectively. The area of the circle for each source is proportional to its flux. The three sources near (-1, -1) are supersoft sources. The 11 sources near (1, 1) and (0, -1) may be unrelated background objects. The cross indicates the mean hardness for all of the sources.

5. CONCLUSIONS

Our high spatial resolution *Chandra* observation of the X-ray–faint elliptical galaxy NGC 4697 resolves most of the X-ray emission (61% within one effective radius) into point sources. A total of 90 individual sources are detected, of which ~80 are LMXBs associated with NGC 4697. Much of the emission is resolved even in the softest band. The dominance of LMXBs implies that this and other X-ray–faint elliptical galaxies have lost most of their interstellar gas.

Of the remaining unresolved emission, it is likely that about half is from fainter LMXBs, while about 23% of the total emission is probably from interstellar gas with $kT \sim 0.3$ keV. Faint, diffuse X-ray emission in the *Chandra* image is asymmetrical and very extended, which also suggests that a portion of the emission is due to hot gas. Ram pressure may have produced the asymmetric feature.

Three of the resolved sources appear to be supersoft sources. Eight of the resolved sources in the outer parts of NGC 4697 (about 25%) are coincident with candidate globular clusters. On the other hand, the candidate globular clusters contain about 0.1% of the optical light of the galaxy in this region. This indicates that globulars have an unusually large fraction of X-ray binaries (by a factor of ~250), as is seen in our Galaxy (e.g., Hertz & Grindlay 1983).

The X-ray luminosities (0.3–10 keV) of the resolved LMXBs range from ~5×10^{37} to ~2.5×10^{39} ergs s^{-1}. The luminosity function has a "knee" at 3.2×10^{38} ergs s^{-1}, which is roughly the Eddington luminosity of a $1.4\,M_\odot$ neutron star (NS). This knee might provide a standard candle that could be used to determine distances to galaxies. This knee may separate accreting NS and black hole (BH) binaries. If the brightest sources in NGC 4697 are Eddington-limited, they must contain fairly massive BHs.

Our detection of a large population of binaries with NSs and massive BHs provides perhaps the most direct evidence that this elliptical galaxy (or its progenitors) once contained a large number of massive main-sequence stars. The population of LMXBs provides a tool to study the high-mass end of the initial mass function of early-type galaxies, long after the massive main-sequence stars have died. The detection of NSs and massive BHs in NGC 4697 also provides the first evidence for the current existence of massive stars (albeit degenerate) in a normal, optically luminous elliptical galaxy.

We are extremely grateful to J. J. Kavelaars for providing his unpublished list of globular clusters in NGC 4697. Bill Harris, J. J. Kavelaars, and Arunav Kundu also gave helpful comments on the globular cluster population of NGC 4697. Support for this work was provided by the National Aeronautics and Space Administration through *Chandra* Award GO0-1019X issued by the *Chandra X-Ray Observatory* Center, which is operated by the Smithsonian Astrophysical Observatory for and on behalf of NASA under contract NAS8-39073. J. A. I. was supported by *Chandra* Fellowship grant PF9-10009, awarded through the *Chandra* Science Center.

REFERENCES

Brandt, W. N., et al. 2000, AJ, 119, 2349
Fabbiano, G., Kim, D.-W., & Trinchieri, G. 1994, ApJ, 429, 94
Faber, S. M., Wegner, G., Burstein, D., Davies, R. L., Dressler, A., Lynden-Bell, D., & Terlevich, R. J. 1989, ApJS, 69, 763
Forman, W., Jones, C., & Tucker W. C. 1985, ApJ, 293, 102
Hanes, D. A. 1977, MmRAS, 84, 45
Hasinger, G., Burg, R., Giacconi, R., Schmidt, M., Trümper, J., & Zamorani, G. 1998, A&A, 329, 482
Hertz, P., & Grindlay, J. E. 1983, ApJ, 275, 105
Irwin, J. A., & Sarazin, C. L. 1998a, ApJ, 494, L33
———. 1998b, ApJ, 499, 650
Irwin, J. A., Sarazin, C. L., & Bregman, J. N. 2000, ApJ, 544, 293
Kahabka, P., & van den Heuvel, E. P. J. 1997, ARA&A, 35, 69
Kim, D.-W., Fabbiano, G., Matsumoto, H., Koyama, K., & Trinchieri, G. 1996, ApJ, 468, 175
Matsumoto, H., Koyama, K., Awaki, H., Tsuru, T., Loewenstein, M., & Matsushita, K. 1997, ApJ, 482, 133
Monet, D., et al. 1998, USNO-A V2.0, a Catalog of Astrometric Standards (Flagstaff: USNO)
Mushotzky, R. F., Cowie, L. L., Barger, A. J., & Arnaud, K. A. 2000, Nature, 404, 459
Pellegrini, S. 1994, A&A, 292, 395
Pellegrini, S., & Fabbiano, G. 1994, ApJ, 429, 105